J. Membrane Biol. 155, 121–131 (1997)

The Journal of
Membrane
Biology

Proton Inhibition of Sodium Channels: Mechanism of Gating Shifts and Reduced Conductance

J.-P. Bénitah[1], J.R. Balser[2], E. Marban[1], G.F. Tomaselli[1]

[1]Section of Molecular and Cellular Cardiology, Johns Hopkins University, 720 North Rutland Ave., Baltimore, MD 21205, USA
[2]Department of Anesthesiology and Critical Care Medicine, Johns Hopkins University, Baltimore, MD 21205, USA

Received: 14 May 1996/Revised: 19 September 1996

Abstract. Extracellular acidosis affects both permeation and gating of the expressed rat skeletal muscle Na^+ channel (μ1). Reduction of the extracellular pH produced a progressive decrease in the maximal whole-cell conductance and a depolarizing shift in the whole-cell current-voltage relationship. A smaller depolarizing shift in the steady-state inactivation curve was observed. The pK of the reduction of maximal conductance was 6.1 over the pH range studied. An upper limit estimate of the pK of the shift of the half-activation voltage was 6.1. The relative reduction in the maximal whole-cell conductance did not change with higher $[Na^+]_o$. The conductance of single fenvalerate-modified Na^+ channels was reduced by extracellular protons. Although the single-channel conductance increased with higher $[Na^+]_o$, the maximal conductances at pH 7.6, 7.0 and 6.0 did not converge at $[Na^+]_o$ up to 280 mM, inconsistent with a simple electrostatic effect. A model incorporating both Na^+ and H^+ binding in the pore and cation binding to a Gouy-Chapman surface charge provided a robust fit to the single-channel conductance data with an estimated surface charge density of $1e^-/439Å^2$. Neither surface charge nor proton block alone suffices to explain the effects of extracellular acidosis on Na^+ channel permeation; both effects play major roles in mediating the response to extracellular pH.

Key words: Sodium channels — Rat skeletal muscle — Fenvalerate — *Xenopus* — Electrophysiology

Introduction

Extracellular acidosis has well-described inhibitory effects on the Na^+ current in nerve, heart and muscle. In studies of whole-cell current, elevation of the external proton concentration produces two consistent effects: a shift in channel gating to more depolarized potentials and a reduction in the maximal Na^+ conductance (Hille, 1968; Woodhull, 1973; Drouin & The, 1969; Campbell, 1982; Begenisch & Danko, 1983; Yatani et al., 1984). The shift in gating has been attributed to titration of negative surface charges accessible from the extracellular surface of the channel. The mechanism of the reduction in Na^+ conductance is less certain. Based on the voltage dependence of proton-induced current reduction, it has been proposed that H^+ enters the pore and binds to a site within the membrane field, producing block (Woodhull 1973; Begenisich & Danko, 1983). However, macroscopic current studies are complicated by the difficulty of separating changes in gating and permeation. In fact, it has been argued on the basis of tail current experiments (Campbell, 1982) that the H^+-induced reduction in conductance is voltage-independent and that the apparent voltage dependence is the result of an effect on channel gating. Extracellular proton-induced inhibition of unitary Na^+ current in guinea pig ventricular myocytes is not voltage-dependent over a wide pH range (Zhang & Siegelbaum, 1991). In contrast, cardiac Na^+ channels that have been modified to remove fast inactivation exhibit a parabolic dependence on voltage with less H^+-induced inhibition of current at the extremes of the voltage range, consistent with proton permeation at negative potentials (Backx & Yue, 1991). Studies of BTX-modified channels reconstituted in planar lipid bilayers also reveal a voltage-dependent reduction in extracellular H^+ inhibition of the Na^+ current at positive voltages (Daumas & Andersen, 1993).

Surface charge reduction or simple titration of a site in the pore by protons does not adequately explain the experimentally observed effects of H^+ on the Na^+ current. We have examined the effect of changes in extracellular pH on skeletal muscle Na^+ channels expressed in

Correspondence to: G.F. Tomaselli

Xenopus oocytes. Acidosis reduces the whole-cell current and shifts the current-voltage relationship to more depolarized potentials. Single-channel recording was used to study the effect of the extracellular pH on Na^+ conductance over a range of $[Na^+]_o$. To avoid the confounding effects of channel gating, patches were modified to remove fast inactivation. Extracellular protons reduce the single-channel conductance in a dose-dependent fashion. This effect is not attenuated at high external Na^+ concentrations and thus is not solely due to a surface charge effect or a simple electrostatic increase in local Na^+ concentration. Proton permeation at negative potentials argues against a simple one-site blocking model.

Some of these data have appeared in abstract form (Bénitah et al., 1995).

Methods and Materials

Channel Expression

Plasmids containing the μ1 Na^+ channel α subunit (Trimmer et al., 1989) and the β1 subunit (Isom et al., 1992) were linearized with *Sal* I and *EcoR* I, respectively for in vitro RNA transcription as previously described (Tomaselli et al., 1991). Oocytes were injected with 50 nl of a 1:1 weight:weight mixture of α and β1 subunit cRNA at a final concentration of 0.1–0.25 μg/μl. Oocytes were harvested from human chorionic gonadotrophin-primed adult female frogs (*Xenopus* I, Ann Arbor, MI or Nasco, Ft. Atkinson, WI). Single oocytes were isolated by digestion of lobes of ovary with 1–2 mg/ml of collagenase (Type IA, Sigma, St. Louis, MO) in modified Barth's solution containing (in mM): 88 NaCl, 1 KCl, 2.4 $NaHCO_3$, 15 tris(hydroxymethyl)aminomethane (TRIS base), 0.3 $CaNO_3 \cdot 4H_2O$, 0.41 $CaCl_2 \cdot 6H_2O$, 0.82 $MgSO_4 \cdot 7H_2O$. The oocytes were stored in modified Barth's solution supplemented with penicillin (100 U/ml) and streptomycin (100 μg/ml), gentamicin (50 μg/ml), sodium pyruvate (2 mM), and theophylline (0.5 mM). Prior to single-channel recording, the visceral vitelline membrane was manually removed after incubation of the oocyte in a hypertonic solution containing (in mM): 220 N-methyl-D-glucamine (NMG), 220 aspartic acid, 2 $MgCl_2$, 10 N-(2-hydroxyethyl)piperazine-N′-(2-ethanesulfonic acid) (HEPES), 10 Ethylene glycol-bis(β-aminoethyl ether)-N, N, N′,N′-tetraacetic acid (EGTA), pH 7.2.

Electrophysiology

Macroscopic currents were recorded using a two-microelectrode voltage clamp (OC-725B Warner Instrument, Hamden, CT) 2–5 days after RNA injection. The resistance of the current electrode was 0.5–1 MΩ and 1–5 MΩ for the voltage-recording electrode when filled with 3 M KCl. Currents were measured in modified frog Ringer's solution containing (in mM): 96 NaCl, 2 KCl, 1 $MgCl_2$, 5 HEPES, with the pH varied between 4.9 and 8.0. For solutions of pH ⩽ 6.5, 2-[N-morpholino]ethanesulfonic acid (MES) replaced HEPES. To optimize voltage control, we used oocytes with small currents (<5 μA). Current records exhibiting an abrupt rise in the negative slope region of the current-voltage relationship or notches were discarded. Steady-state inactivation was determined using 200 millisecond prepulses ranging from −110 to −30 mV in decrements of 5 mV preceding a test pulse to −20 mV. To avoid cumulative inactivation, a repetition interval of 4 sec was employed. We observed no voltage shift in the steady-state inactivation curves over the time course of these experiments (up to 45 min). Whole-cell current were sampled at 5 kHz through a 12 bit A/D converter (model TL-1 DMA Labmaster, Axon Instruments, Foster City, CA) and lowpass filtered at 1–2 kHz (−3 dB) with an 8-pole Bessel filter (Frequency Devices, Haverhill, MA). The currents were acquired and analyzed using custom-written software.

Single-channel currents were measured using the cell-attached patch clamp configuration (Hamill et al., 1981) with an Axopatch 200A amplifier (Axon Instruments, Burlingame, CA). The currents were sampled at 10 kHz and low-pass filtered at 1 kHz. The pipette solution contained (in mM): 140 NaCl, 10 HEPES (or MES, pH 6.0), 1 $BaCl_2$, and the bath contained (in mM): 140 KCl, 10 HEPES (or MES, pH 6.0), the pH of the pipette and bath solutions were changed symmetrically. Single-channel currents were recorded between pH 6 and 8, below pH 6 patch stability was severely compromised. Junction potentials were zeroed prior to patch formation. The unitary currents were modified by bath application of 20 μM fenvalerate (DuPont, Wilmington, DE) to prolong openings and thereby facilitate analysis of the effects of changing the extracellular pH on permeation (Holloway et al., 1989; Backx et al., 1992). All experiments were performed at 20–22°C.

Data Analysis

Whole-cell current-voltage relationships were fit with a function combining the Boltzmann distribution describing steady-state activation and the Goldman-Hodgkin-Katz constant field equation (Hille, 1992): $I/I_{max} = (V - V_{rev})\, G_{max}/\{[1 + exp[(V - V_{0.5})/k]] + 1\}$, where V is the test potential, and the parameters estimated by the fit where V_{rev}, the reversal potential; G_{max}, the relative maximal conductance; $V_{0.5}$, the half point of the relationship; and k, the slope factor. Because of underestimation of the peak current at positive test potentials only currents elicited by voltage steps to 0 mV or less were fit.

Steady-state inactivation curves were generated using a two-pulse protocol and the normalized peak currents were fit with a Boltzmann function: $I/I_{max} = \{1 + exp[(V_{0.5} - V)/k]\}$, where V is the potential of the conditioning pulse, $V_{0.5}$, the potential at which the current is half-maximally inactivated, and k, the slope factor. The best-fit curves to the data were determined using a nonlinear least squares method (Levenberg-Marquardt algorithm, Origin, MicroCal, Northhampton, MA). We made no assumptions about the number of titrable sites hence, the pH dependence of the activation voltage shift was fit with a function of the form: $\Delta V_{0max}/[1 + 10^{(pKa-pH)n}]$, where ΔV_{0max} is the maximal shift of the activation voltage and n is the slope of the curve. The pH dependence of the normalized maximal conductance was fit with the function $1/[1 + 10^{(pKa-pH)n}]$. The dependence of the maximal conductance on $[Na^+]_o$ was fit with a saturating single-site binding model.

Single-channel analysis was performed using custom-written software. Single-channel opening events were determined using a half-height criterion (Colquhoun & Sigworth, 1983). Amplitude histograms were fitted to the sum of Gaussians using a nonlinear least squares method. Pooled data are expressed as the means and standard deviations, and statistical comparisons were made using one-way ANOVA unless otherwise specified.

Model

We have modeled the effects of varying concentrations of H^+ and Na^+ on Na^+ conductance by including three modulating features: surface charge screening, specific binding of Na^+ and H^+ to surface charges, and block of the pore by H^+. For simplicity, we have assumed that the Na^+ conductance at an infinitely low H^+ concentration (γ_{Na}) is linear

with respect to voltage over the range we consider in our analysis. We assume that at 1 mM $BaCl_2$ acts to screen surface charge. There is no evidence that Ba^{2+} acts as a competitive blocker of the channel. Further, we assume that γ_{Na} is a saturable function of Na^+ binding to a single site in the pore with a dissociation constant K_{NaP} as follows:

$$\gamma_{Na} = \gamma_{max}/[(K_{NaP}/[Na^+]_P) + 1] \quad (1)$$

where γ_{max} is the maximum Na^+ conductance and $[Na^+]_P$ is the Na^+ concentration at the entrance to the pore, corrected for surface potential effects on local ion concentration. We include a term for H^+ binding to a single site in the pore to block the Na^+ conductance (Zhang & Siegelbaum, 1991), thus the Na^+ conductance at any H^+ concentration ($\gamma_{Na/H}$) may be defined as follows:

$$(\gamma_{Na/H} = \gamma_{Na}/[([H^+]_P/K_{HP}) + 1] \quad (2)$$

where $[H^+]_P$ is the hydrogen ion concentration at the pore surface, corrected for the concentrating effect of the surface potential, and K_{HP} is the dissociation constant of blocking site in the pore for hydrogen ions. It is assumed that proton block occurs on a rapid time scale, thereby causing an apparent reduction in the unitary current amplitude, translating into a reduction in $\gamma_{Ha/H}$. Eqs. (1) and (2) may be combined into a single expression for $\gamma_{Na/H}$ as follows:

$$\gamma_{Na/H} = \gamma_{max} \cdot [(K_{NaP}/[Na^+]_P) + 1]^{-1} \cdot [([H^+]_P/K_{HP}) + 1]^{-1} \quad (3)$$

The Na^+ and H^+ concentrations at the pore surface may be corrected for the surface potential using the Boltzmann equation:

$$[H^+]_P = [H^+]_B \, exp(-z\Phi F/RT) \quad (4)$$

$$[Na^+]_P = [Na^+]_B \, exp(-z\Phi F/RT) \quad (5)$$

where $[H^+]_B$ and $[Na^+]_B$ are the bulk concentrations of protons and Na^+ respectively, z is the cation valence, Φ is the surface potential, and RT/F = 25.3 mV at 20°C.

The surface potential is related to a uniform planar surface charge (σ_a) in an electrolyte solution by Gouy-Chapman theory. The screening effect of ions on the surface charge is given by the Grahame equation (Grahame, 1947) as follows:

$$\sigma_a^2 = G^{-2} \{[Na^+]_B \cdot (exp(\Phi F/RT) - 1) + [H^+]_B \cdot (exp(\Phi F/RT) - 1)\} \quad (6)$$

where G = 270 $Å^2 e^{-1} M^{0.5}$, giving an apparent surface charge density (σ_a) in units of $e^-/Å^2$. Specific association of the cations with the surface charge allows expression of the apparent surface charge as a function of the total surface charge (σ_t) as follows:

$$\sigma_a = \sigma_t \{1 + [Na^+]_B K_{NaM} \, exp(-z_i\Phi F/RT) + [H^+]_B K_{HM} \, exp(-z_i\Phi F/RT)\} \quad (7)$$

This equation assumes that the same surface charges bind Na^+ and H^+, but not necessarily with the same affinity. The voltage dependence of block is implicit in the model in the conductance term. We assume that the electrical distances do not change at different pHs. For any particular $[Na^+]_B$ and $[H^+]_B$, Eqs. (6) and (7) may be used to calculate the surface potential (Φ), from which the local ion concentrations can be calculated and then used to solve Eq. 3. Hence, there are six unknown parameters relating the conductance $\gamma_{Na/H}$ to $[Na^+]_B$ and $[H^+]_B$:

K_{NaM}, K_{HM}: association constants of the surface charge for Na^+ and H^+ respectively (M^{-1})

K_{NaP}, K_{HP}: dissociation constants of the pore for Na^+ and H^+ respectively (M)

σ_t: total membrane surface charge ($e^-/Å^2$)

γ_{max} = maximum Na^+ conductance in the absence of H^+ ions (pS).

To determine values for these parameters, initial guesses were made and surface potential was determined using a numerical bisection method (Press et al., 1992). With this initial value of surface potential, the Na^+ conductance was calculated using Eq. 3. A simplex algorithm (Nelder & Mead, 1965) was then used to compare the calculated Na^+ conductance to the measured value, and iteratively modify the parameters to minimize the sum-of-squared error. The importance of specific features of the model were then evaluated by fitting subsets of the complete model to the data. The sum-of-squared error was compared to that obtained using the complete model using an F ratio (Horn, 1987).

Results

Protons Shift Gating of Expressed Na^+ Channels

The μ1 skeletal muscle Na^+ channel expresses robustly in *Xenopus* oocytes with rapid decay kinetics in the presence of the β1 subunit (Nuss et al., 1995). External protons decrease whole-cell Na^+ current and shift the current-voltage (*I–V*) relationship to more depolarized potentials. Figure 1*A* shows normalized *I–V* relationships for currents recorded from thirty oocytes at three different pHs. The *I–V* relationships at a given pH are normalized to that at pH 7.6 and are fit with a function combining the Goldman-Hodgkin-Katz current equation and the Boltzmann relationship to estimate maximal conductance (G_{max}) and the voltage for half-activation (V_0). The pH dependence of the maximal conductance reflects proton-induced changes in permeation since the G_{max} measurement compensates for gating shifts. Under the reference conditions (pH 7.6, 0 Ca^{2+}, 1 mM $MgCl_2$), the expressed channels begin to activate at −60 mV, the peak current is observed at −35 mV and the fitted half-maximal activation voltage is −46 mV. Small changes in the *I–V* relationship are observed at pH 7.0 compared with pH 7.6. The current at pH 7.0 activates at −55 mV, with the negative slope region of the *I–V* shifted approximately +5 mV compared to the *I–V* at pH 7.6. The *I–V* peaks between −30 and −35 mV and is half-maximally activated at −43 mV. The maximal conductance at pH 7.0 is decreased approximately 10% from the reference condition. The Na^+ current recorded from the same oocytes at pH 6.0 had a dramatically shifted *I–V* relationship and a greater than 50% reduction in the maximal conductance. The current at pH 6.0 activates at −45 mV, peaks at −20 mV and is half-maximally activated at −31 mV. At pH 5.0 the whole-cell current is not measurable under these recording conditions. Under our whole-cell recording conditions, assuming an intracellular Na^+ concentration in the oocyte of about 10 mM the equilibrium

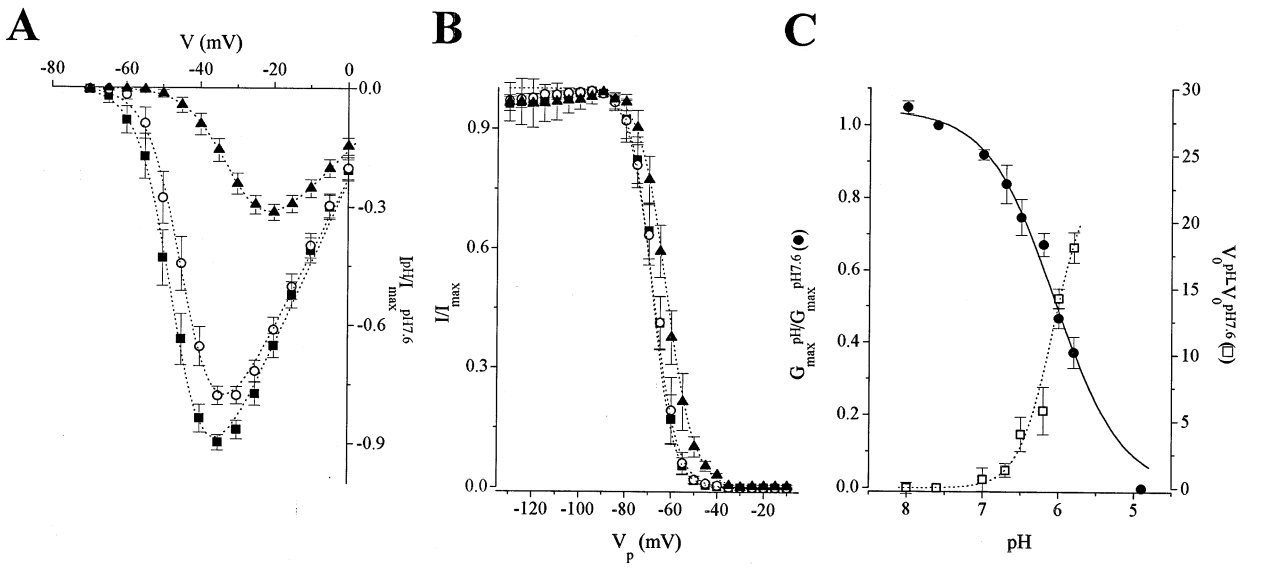

Fig. 1. The effect of extracellular acidosis on expressed skeletal muscle Na^+ channels. Whole-cell currents recorded from *Xenopus* oocytes expressing the μ1 Na^+ channel α subunit and the rat brain β1 subunit. The cells are held at −100 mV and currents are elicited by 50 msec voltage steps from −70 to 0 in increments of 5 mV. (*A*) Normalized *I-V*s from 30 oocytes at pH 7.6 (■), 7.0 (○), and 6.0 (▲) the data are fit by a function combining the Boltzmann distribution describing steady-state activation and the Goldmann-Hodgkin-Katz constant field equation (Hille, 1992). The estimated half-activation voltage and the voltage eliciting the peak current are shifted to the right. The maximal conductance is reduced more than 50% at pH 6.0 compared to that at 7.6. (*B*) The steady-state availability curves at pH 7.6, 7.0 and 6.0 (same symbols as panel *A*) generated by 200 msec prepulses to the designated potentials (−140 to −10 mV in 5 mV increments) followed by a 50 msec test pulse to −35 mV. Each of the curves represents the mean and standard deviation from 6 oocytes. The half-inactivation voltage is unchanged at pH 7.0 compared with that at pH 7.6 (−68.2 ± 0.6 mV *vs.* −68.4 ± 0.6 mV), a significant shift (half-inactivation voltage of −62.3 ± 0.6 mV) was observed at pH 6.0. (*C*) pH-dependent shift in the half-activation voltage and maximal conductance. The activation voltage shift (open squares) referenced to pH 7.6 between pH 5.8 and 8.0 has an estimated pK of 6.1 ± .11 fit to a single-site titration model (broken line). Each data point represents data from at least seven oocytes. A plot of the maximal conductance (solid squares) determined from the fits of the whole-cell *I-V* normalized to the G_{max} at pH 7.6. The fit (continuous line) of the data give a pK of 6.1 ± .03. The pH dependence of whole-cell gating and maximal conductance are similar.

potential for Na^+ is approximately +56 mV. Comparisons of the reversal potentials of currents recorded in the whole-oocyte configuration are difficult because of the large capacity transient and the speed of the currents at positive test voltages near E_{Na}. Therefore only the whole-cell current elicited by voltages steps to less than 0 mV were fit.

The rate of the effect of changing the extracellular pH on both the voltage-dependence of gating and the peak current amplitude is limited by the exchange rate of the bath. The current amplitude decreases and reaches a new steady-state within seconds of perfusing the bath with an acidic solution; the increase in the peak current with washout is equally rapid (*data not shown*). Increasing the extracellular proton concentration did not change the holding current, arguing against a substantial inward H^+ current. The rapid kinetics of the pH-induced changes in the whole-cell current and the absence of a significant depolarization of the cells suggest that the effect is not due to a change in the intracellular pH.

The steady-state availability of the Na^+ current is modulated by extracellular pH. At pH 7.0 or greater there was no shift in the midpoint of the steady-state inactivation curve compared to the reference condition. The curves at pH 7.6 and 7.0 are superimposable, with half-inactivation voltages of −68.4 and −68.2 mV and slope factors of 4.7 and 5.2 mV respectively. No statistically significant difference was observed for the mean values in either $V_{0.5}$ (in mV: −66.2 ± 16.1 pH 7.0 [n = 8]; −66.9 ± 9.5 mV at pH 7.6 [n = 16]; P = NS), or k (in mV: 3.9 ± 0.3 *vs.* 4.0 ± 0.2 mV, P = NS, pH 7 *vs.* pH 7.6 respectively). At lower extracellular pH the availability curve shifts in the depolarizing direction and the slope factor increases. The half-maximal availability voltage and slope factors are −62.3 and 6.0 mV respectively at pH 6.0 (Fig. 1*B*). The same analysis repeated in thirteen different oocytes gave mean values of −63.4 ± 10.2 mV for $V_{0.5}$ ($P < 0.01$ *vs.* pH 7.6), and 4.1 ± 1.4 mV for k (P = NS *vs.* pH 7.6).

Comparison of the Shifts in Gating and the Maximal Conductance

Figure 1*C* compares the pH dependence of the activation gating shift and maximal whole-cell conductance. Whole-cell currents were measured between pH 5.8 and 8.0. The squares represent the difference between the

Table 1. Ratio of whole-cell conductances at pH 7.0 and 6.0

$G^{pH}_{max}/G^{7.6}_{max}$	$[Na^+]_o$ 140 mM $n = 12$	$[Na^+]_o$ 96 mM $n = 30$	$[Na^+]_o$ 58 mM $n = 10$
pH 7.0	0.87 ± 0.1	0.92 ± 0.1	0.92 ± 0.04
pH 6.0	0.44 ± 0.2	0.47 ± 0.15	0.52 ± 0.1

half-activation potentials at the test pH and the reference pH, 7.6. There is an insignificant shift in the half-activation potential at pHs greater than 7.0, but the magnitude of the shift increases at higher $[H^+]_o$ with an estimated pKa of 6.1 ± 0.1. The voltage shift of the peak inward current has a similar pH dependence and pKa (*data not shown*). The reduction in Na^+ current below pH 5.8 precludes accurate determination of the voltage shift. The maximal whole-cell conductance does not increase significantly above pH 7.6 and falls most steeply between pH 7 and 5. The maximal conductance normalized to that at pH 7.6 decreases with increased extracellular proton concentration with a pKa of 6.1 ± 0.03 (Fig. 1*C*, circles), a value close to the estimated pKa for the voltage shift. Extracellular acidosis reduces conductance and shifts the activation voltage to more positive potential. The proton-induced changes in conductance and gating could be due to a parallel dependence on screening surface charge, or titrating a single class of negative charges.

To determine whether titrating external negative charges influences conductance by an electrostatic mechanism, we examined the pH dependence of the whole-cell conductance at different external Na^+ concentrations. The maximal conductance is determined from fits of the normalized *I–V*s at 58, 96, and 140 mM $[Na^+]_o$, such that the relative maximal conductance (relative G_{max}) is unitless. The relative maximal conductances are all in the limiting slope region of the Michaelis-Menten fit, well below the estimated K_ms. The ratio of conductances do not converge over the range of $[Na^+]_o$ studied (Table 1); in fact, at pH 6.0 the conductance at 140 mM $[Na^+]_o$ is smaller than that at 58 mM normalized to the reference conditions, pH 7.6. This failure of convergence may reflect the genuine absence of an electrostatic effect; alternatively, convergence may be seen only at higher Na^+ concentrations. However, limitations in voltage control preclude the study of whole-cell current in oocytes at higher external Na^+ concentrations. It is likely that, even if a surface charge binding or screening effect is present, protons also alter conductance in the Na^+ channel by other mechanisms. We employed single-channel recording to study the effects of protons on the open-channel properties.

Reduction of Single-Channel Current by Protons

External protons affect both the open probability and the unitary Na^+ conductance. To study the effect of acidosis on Na^+ permeation, membrane patches were modified with fenvalerate to remove fast inactivation and promote long, uninterrupted openings. Modification of the Na^+ channel with fenvalerate does not change the conductance. Figure 2 (top) illustrates single-channel openings in the absence and presence of 20 μM fenvalerate at test potentials of −50 and −30 mV; the unitary current amplitude does not change. The *i–V* relationships of the channel before and after modification are superimposible (Fig. 2, bottom).

Figure 3*A* illustrates representative single-channel tail currents elicited by depolarizations to −20 mV followed by repolarizing steps to potentials from −80 to −20 mV in increments of 20 mV at pH 7.6, 7.0, and 6.0. Openings in the tails were analyzed only if an opening was observed in the depolarizing test pulse to avoid contamination of the amplitude histograms with stretch-activated cation channels commonly observed in oocyte membrane patches. At pH 7.6, tail currents exhibit well-resolved openings tens of milliseconds in duration with little intrinsic gating. A monotonic reduction in the current amplitude and an increase in the open-channel noise are observed over all voltages at pH 6.0 and 7.0 compared with pH 7.6. The appearance of the unitary current records is reminiscent of rapid open-channel block (Hille, 1992). The average single-channel current amplitude at each potential was determined by fitting amplitude histograms composed of well-resolved openings. The single-channel current-voltage relationship in 140 mM $[Na^+]_o$ (Fig. 3, bottom) reveals slope conductances of 37, 34 and 23 pS at pH 7.6, 7.0 and 6.0 respectively.

Single-channel current-voltage relationships over a wider range of potentials at 96 mM external Na^+ are shown in Fig. 4*A*. The single-channel conductances measured over the same voltage range at all pHs are reduced compared to the current recorded in higher external Na^+. At the most negative voltages, the single-channel current is sublinear at pH 7.6 and 7.0, likely reflecting a combination of block of the channel by Ba^{2+} and proton permeation at negative potentials (Sheets & Hanck, 1992). At pH 6, the *i–V* is linear or slightly superlinear, consistent with proton permeation and/or multi-ion occupancy of the pore. The voltage dependence of the current reduction by extracellular protons was measured by comparing the single-channel current amplitudes at pH 7.0 and 6.0 to that at pH 7.6. A plot of the ratio of the current amplitudes at both pH 7.0 and 6.0 reveals no voltage-dependent block: the curves are flat over the voltage range of −80 to 0 mV (Fig. 4*B*). These results are comparable to similar measurements in the same voltage range in reconstituted rat brain Na^+ channels (Daumas & Andersen, 1993) and guinea pig ventricular myocytes (Zhang & Siegelbaum, 1991; Backx & Yue, 1991). At pH 6, the single-channel current ratio increases at test potentials below −80 mV, an effect that

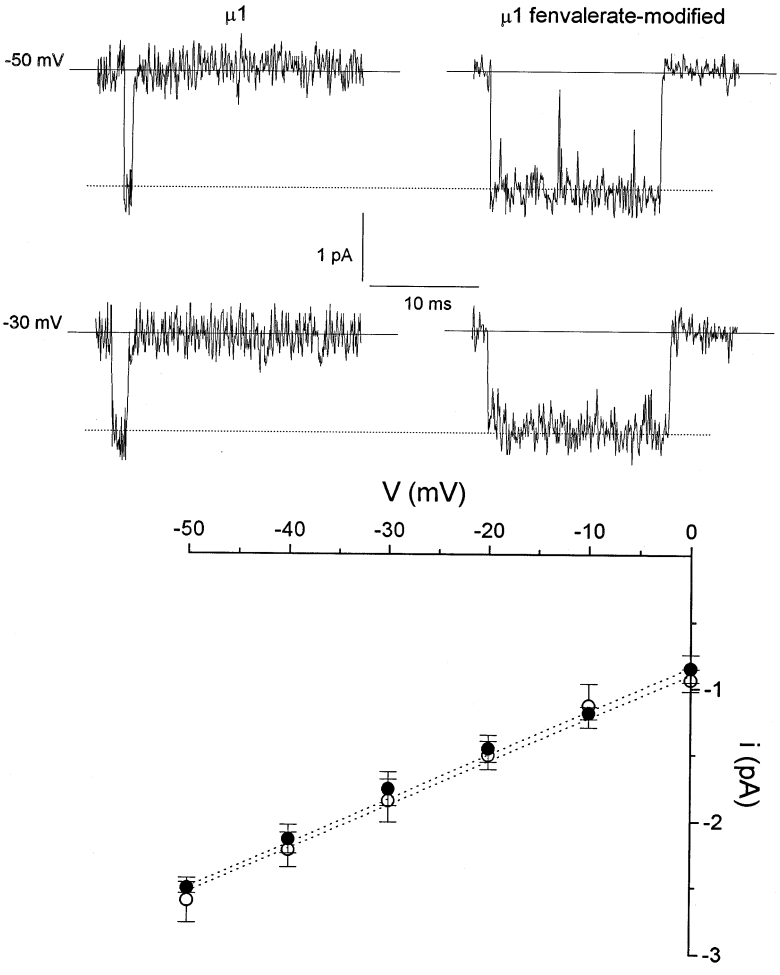

Fig. 2. Fenvalerate does not alter the single-channel conductance. (top) Unitary current records elicited by step depolarizations to −50, and −30 mV in the absence (left) and presence of 20 μM fenvalerate (right). (bottom) The single-channel current-voltage relationship for control (open circles) and fenvalerate-modified (filled circles) channels. The curves represent the mean and standard deviation from five membrane patches, the slope conductances between 0 and −50 mV is 32.9 ± 1 (control) and 33.3 ± 1.4 pS (fenvalerate-modified).

has been observed in native cardiac Na^+ channels (Backx & Yue, 1991) and is inconsistent with a simple proton blocking model without proton permeation (Woodhull, 1973).

The voltage shift of the whole-cell gating parameters by external protons suggests a reduction in surface potential. To determine if the decrease in single-channel conductance at low pH is the result of a surface charge effect, we measured the single-channel current over a broad range of $[Na^+]_o$. Titration of a negative surface charge could decrease conductance by an electrostatic reduction in the local Na^+ concentration; this mechanism predicts that increasing the extracellular bulk $[Na^+]$ should restore the conductance at low pH (Green et al., 1987). The concentration-conductance relationships at all pHs should converge at high $[Na^+]_o$. Figure 5*A* and Table 2, which show results at pH 7.6, 7.0 and 6.0 over a range of $[Na^+]_o$ from 58 to 280 mM illustrate that this is not the case. The conductances at the highest permeant ion concentration do not converge, suggesting that changing the pH alters the γ_{max}. The effect of external acidosis on permeation is not explained by changes in surface charge alone; it appears that protons fundamentally alter the energy profile experienced by Na^+.

In cardiac ventricular myocytes it has been suggested that titration of a single class of acidic blocking sites is responsible for the proton-induced decrease in single-channel conductance (Zhang & Siegelbaum, 1991). Figure 5*B* shows the single-channel conductance in 140 mM $[Na^+]_o$ from pH 6–8. The fit of the data to a one-site binding model (*broken line*) predicts a steeper slope of the conductance-pH relationship than is observed. Simple titration of a carboxylate(s) or any single class of negative sites does not appear to explain the reduction in single-channel conductance produced by $[H^+]$ in expressed skeletal muscle Na^+ channels.

Model

To refine our understanding of the effects of pH and $[Na^+]_o$ on conductance in the Na^+ channel, we have generated a model that considers surface charge screening, specific binding by Na^+ and H^+ to surface charges, and

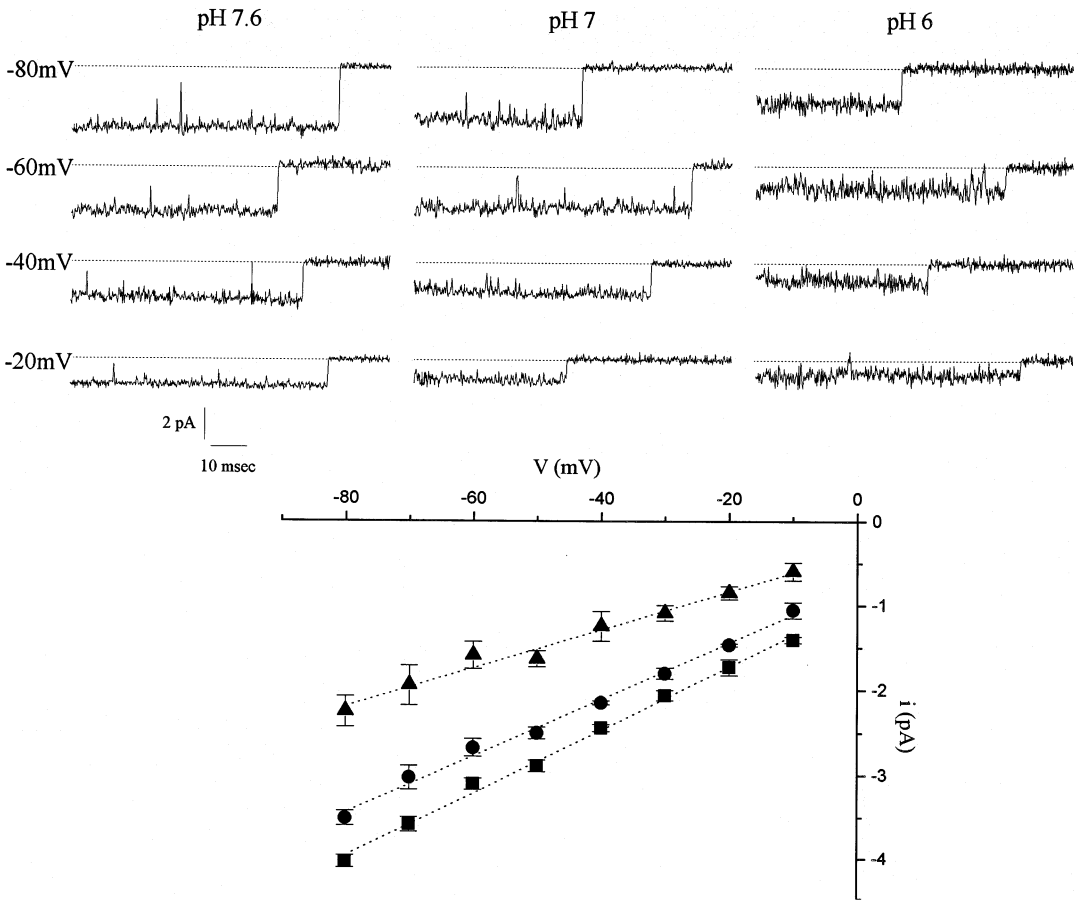

Fig. 3. Single-channel current reduction by extracellular protons. Single-channel current records from fenvalerate modified cell-attached patches with 140 mM Na^+ in the pipette. The single-channel current is reduced and the open-channel noise increases with reduction in the extracellular pH giving the appearance of rapid open channel block. The single-channel current-voltage relationships at pH 7.6 in eleven patches, 7.0 in six patches, and 6.0 in five patches reveals slope conductances 37.3 ± 1.0, 33.4 ± 1.1, and 22.6 ± 1.3 pS respectively.

pore block of the Na^+ channel by protons (*see* Materials and Methods). Because of the limitations in the analysis of the whole-cell data the model was only fit to the single-channel data. The entire data set of single-channel conductances at all $[Na^+]_o$ and pH 6, 7, and 7.6 were fit by the model. The full model can be constrained to test the relative importance of surface charge effects and pore binding of protons on the Na^+ conductance. In Fig. 6*A*, model 1 considers only titration and screening of surface charge by protons and Na^+; deficiencies of this model are visibly apparent at all $[Na^+]_o$ and over the entire pH range. Elimination of surface charge titration by protons and modeling the effects of acidosis entirely by binding in the pore provides a fit (model 2) that is improved over the model that incorporated surface charge alone, but systematic errors are observed at the lowest and highest $[Na^+]_o$. If the same sites or class of sites account for the surface charge and the pore binding of H^+, then similar affinities for proton binding at the membrane and in the pore are expected. If the model incorporates both titration of surface charge and binding to a pore site by protons but with the same affinity, the fit (model 3) is marginally improved over those which do not consider both surface charge and pore binding. Model 4 in Fig. 6*A* removes the constraint of equal affinities in model 3 and incorporates all of the parameters. Model 4 provides the most robust fit (SSE: model 1 = 56, model 2 = 26, model 3 = 22, model 4 = 10; $P < 0.05$ in pairwise comparisons) and predicts a total surface charge density of $1e^-/439$ Å^2, a pK_a for H^+ binding in the pore of 5.7, and a K_d for Na^+ binding of 160 mM.

To explore further the adequacy of the constrained versions of the general model (model 4), we examined the pH dependence of Na^+ conductance over a wider range at one $[Na^+]_o$ (140 mM). Deviations of the fits provided by some of the constrained versions of the model become more obvious at higher pH. To highlight the differences among the model predictions, we plotted the conductance data at 140 mM $[Na^+]_o$ between pH 7 and 8 fit with each of the models. Models 1–3 (Fig. 6*B*)

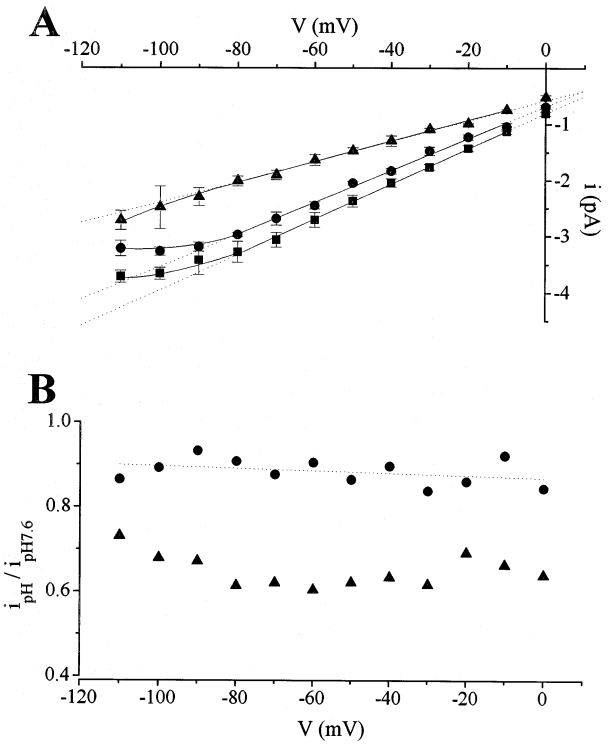

Fig. 4. Voltage-dependence of the reduction of single-channel current by protons. (*A*) The single-channel current voltage relationship in 96 mM Na^+ at pH 7.6 (squares), 7.0 (circles) and 6.0 (triangles). The slope conductance (broken line) decreases monotonically with pH over this range. At negative voltages the *i-V* is sublinear at pH 7.6 and 7.0 and supralinear at pH 6.0. (*B*) The ratio of the single-channel current amplitude at pH 7.0 (circles) and 6.0 (triangles) compared to pH 7.6. At pH 7.0 the ratio of unitary current amplitudes is flat over the voltage range 0 to −110. At pH 6.0 the current ratio is voltage dependent over the range of voltages from −80 to −110 mV but the voltage dependence is opposite that predicted for simple block of the pore.

underestimate the conductance at pH 8 and have significantly larger sums of squared error than model 4 ($P < 0.001$, in pairwise comparisons). The model which eliminates surface charge is particularly poor at this $[Na^+]_o$ at pH > 7 (Fig. 6*B*, model 2). Inclusion of all the parameters provides the best fit over the entire pH range studied (Fig. 6*B*, model 4).

Discussion

The effect of pH on expressed skeletal muscle Na^+ channels is similar to that observed in native channels in nerve, heart and skeletal muscle (Hille, 1968; Campbell, 1982; Yatani et al., 1984). The macroscopic current is reduced and voltage-dependent gating is shifted to more depolarized potentials at lower pH. We focused on the mechanism of proton-induced reduction in Na^+ conductance by studying single Na^+ channels modified to remove fast inactivation. External protons decrease the single-channel current amplitude and increase the open-channel noise in a voltage-independent fashion. Neither titration (or screening) of an external Gouy-Chapman-Stern surface charge nor proton block in the pore alone suffices to explain the effect of external acidosis on Na^+ conductance; however, a model incorporating both effects robustly fits our single-channel conductance data over a range of $[Na^+]_o$ between pH 6 and 8.

Effects on the Whole-Cell Current

The peak macroscopic current is reduced in the presence of elevated concentrations of external protons. The G_{max} is half-maximal at pH 6.1 and is near zero at pH 4.8 (Fig. 1*C*). There is a parallel shift in the voltage dependence of gating (V_0) over a similar pH range, although the current reduction at low pH precludes definition of the maximal voltage shift. An upper limit estimate of the pKa of the whole-cell voltage shift is 6.1. A similar pH dependence for gating shifts and conductance has been described for cardiac myocytes (Yatani et al., 1984; Zhang & Siegelbaum, 1991). Zhang and Siegelbaum attribute the similar pH dependence of single-channel gating and conductance to titration of a single class of sites by external protons (Zhang & Siegelbaum, 1991). The pH dependence of the whole-cell conductance and of the expressed human cardiac Na^+ channel, hH1 (*data not shown*) was similar to that of μ1, suggesting that conserved residues mediate the effect of external pH on the current.

The G_{max} could be reduced by protons that titrate negative sites on the external face of the channel thereby reducing the local Na^+ concentration and driving force for Na^+ permeation. This mechanism predicts that the effect of a lower pH should be overcome by increasing the bulk Na^+ concentration. In fact, there is no convergence of the G_{max} at pH 7.6, 7 and 6 at higher $[Na^+]_o$ (Table 1); this observation is inconsistent with a simple electrostatic mechanism of proton reduction of Na^+ current. However, we did not attempt to draw any mechanistic conclusions from the whole-oocyte experiments, and relied on the single-channel current measurements for interpreting the effect of extracellular protons on permeation.

Effects of External Protons on Single-Channel Conductance

We studied the effects of pH on the isolated, open conformation of the Na^+ channel by removing fast inactivation, thereby removing the confounding effects of gating. The appearance of the unitary Na^+ currents at low pH suggests rapid open-channel block with a reduction in current amplitude and an increase in open-channel noise.

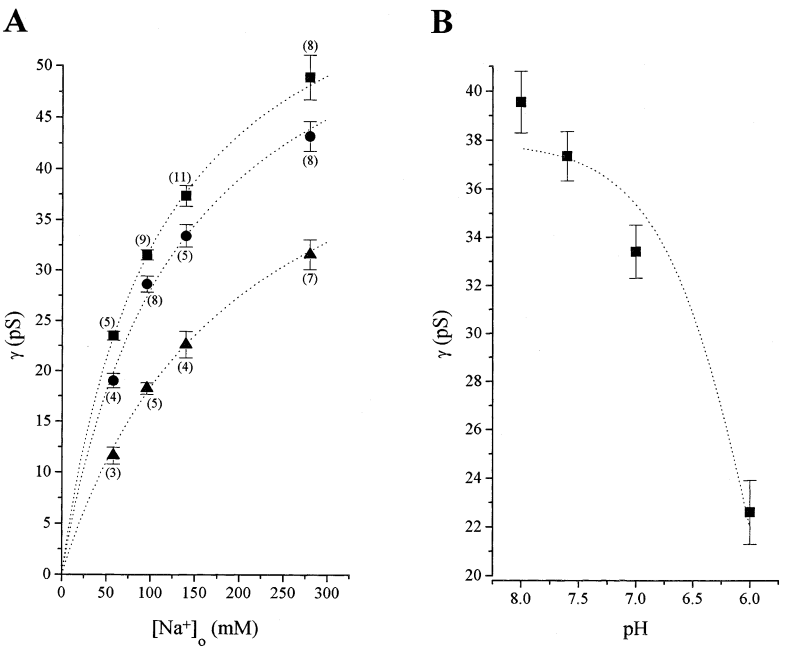

Fig. 5. (*A*) Single-channel conductance as a function of $[Na^+]_o$ at pH 6.0 (triangles), 7.0 (circles) and 7.6 (squares). A plot of single-channel conductance measured in at least three patches over a range of $[Na^+]_o$ from 48 to 280 mM. The points are connected for clarity; the number of patches for each data point is given in the parentheses. The ratio of the conductances in 280 mM $[Na^+]_o$ at pH 7.0 and 6.0 compared to that at pH 7.6 are 0.98 and 0.64. The curves do not converge over this permeant ion concentration range. (*B*) Dose-response curve of the inhibition of the single-channel Na^+ current by external H^+. The conductances were measured with an $[Na^+]_o$ of 140 mM and each data point represents at least five patches. The broken line is a fit of the data to a single-site titration model and yields an estimated pKa of 5.9 ± 0.1.

Table 2. Ratio of single-channel conductances at pH 7.0 and 6.0

$\gamma^{pH}_{max}/\gamma^{7.6}_{max}$	$[Na^+]_o$ 280 mM	$[Na^+]_o$ 140 mM	$[Na^+]_o$ 96 mM	$[Na^+]_o$ 58 mM
pH 7.0	0.88	0.89	0.91	0.81
pH 6.0	0.64	0.60	0.58	0.49

The simplest model of pore block is contradicted by the absence of voltage dependence of proton block (Fig. 4*B*). The voltage independence of the current reduction has been explained by invoking permeation by protons (Beginisich & Danko, 1983), which our data cannot exclude. Zhang and Siegelbaum have suggested that protons titrate negative charges on the channel surface, decreasing the local $[Na^+]$ and current in a voltage-independent fashion (Zhang & Siegelbaum, 1991). Our single-channel conductance data are not well fit by a single-site titration curve (Fig. 5*B*). Further, the effect of reduction of surface potential by a lower pH should be mitigated by increasing the bulk $[Na^+]_o$, producing converging conductance-Na^+ concentration relationships at all pHs. This is not the case for the expressed skeletal muscle Na^+ channel in which maximal single-channel conductances measured between pH 6 and 7.6 show no evidence for convergence (Fig. 5*A*, Table 2). This failure of convergence implies that protons may be having a more fundamental effect on the energy profile experienced by permeant Na^+.

To assess the contribution of surface charge and pore block on the proton-induced reduction in Na^+ conductance, we fit our single-channel data with a model that considers binding and screening of surface charge by both protons and Na^+, and block of the pore by H^+. The fits of the models to our complete data set suggest that there are components of titration and/or screening of surface charge and pore block operative in the proton-induced decrease of the single-channel Na^+ conductance. Model 4 includes all of the parameters and yields the best fit to the data (Fig. 6*A*). The total surface charge density derived from this model is $1e^-/439$ Å^2, similar to estimates from other Na^+ channel preparations (Ravindran & Moczydlowski, 1989; Chabala & Anderson, 1989; Zhang & Siegelbaum, 1991). Eliminating the surface charge (model 2) or pore binding of H^+ (model 1) produces systematic errors in the fits that are exaggerated at high pH (Fig. 6). If both surface charge and H^+ binding in the pore are incorporated but constrained such that the affinity for binding to surface charge and the pore site are identical, the goodness of the fit is reduced compared to the fully parameterized model. Our interpretation of the modeling is that, at a minimum, both surface charge binding and screening and intrapore H^+ block are required to explain the effects of Na^+ and protons on single-channel conductance. The lack of voltage dependence of H^+ block may imply that the proton binding site is near the edge of the transmembrane voltage gradient. It does not appear that a single class of negatively charged sites which control the $[Na^+]_o$ by a surface charge mechanism adequately explains the proton-induced alterations in conductance observed in expressed skeletal muscle Na^+ channels.

The reduction in whole-cell conductance tracks the reduction in single-channel conductance at low pH (Tables 1 and 2). The effect of acidosis on the whole-cell conductance appears to result primarily from a re-

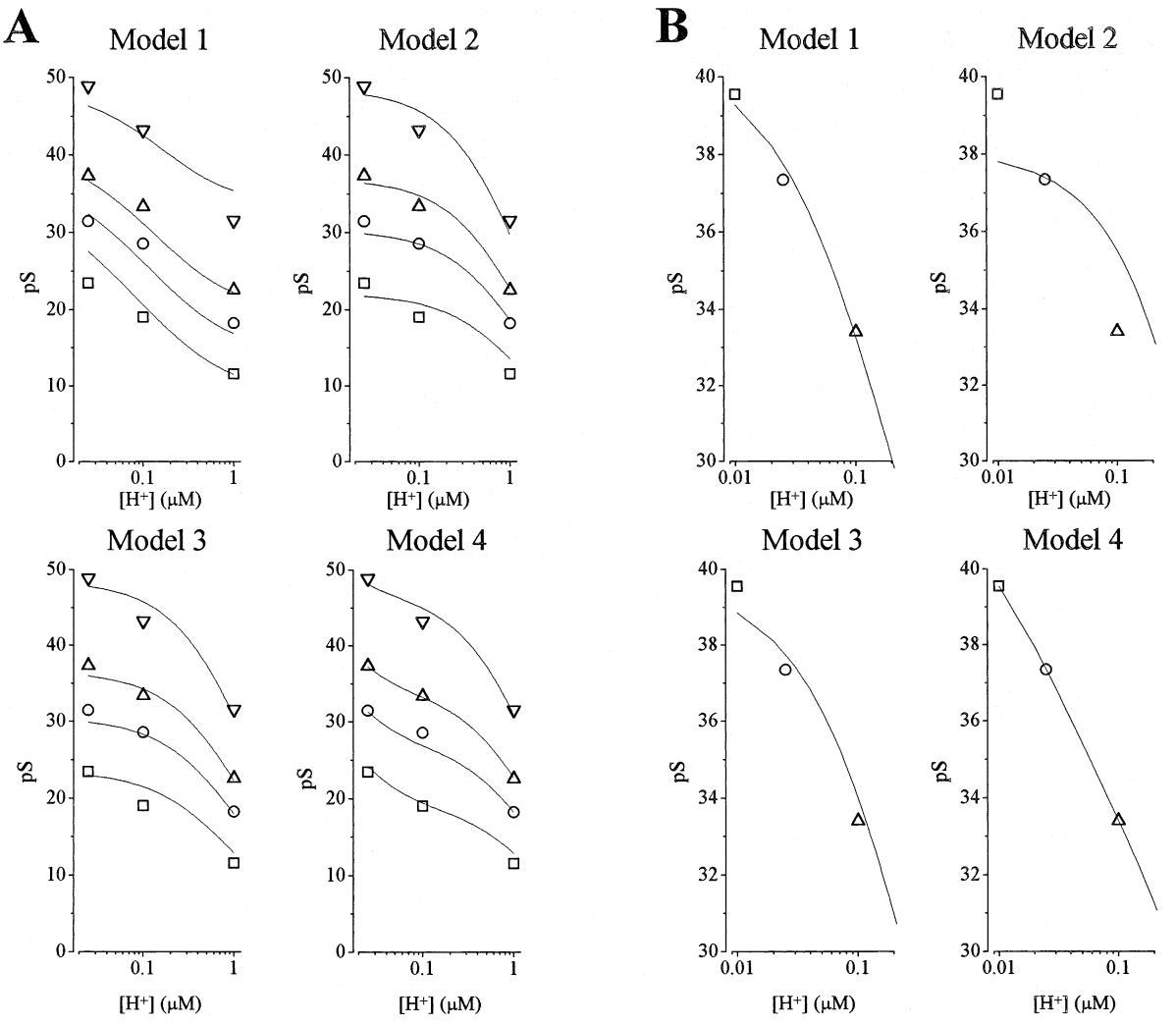

Fig. 6. pH and Na^+ dependence of the single-channel conductance. (*A*) Plots of conductance *vs.* proton concentration at $[Na^+]_o$ of 58 mM (squares), 96 mM (circles), 140 mM (triangles) and 280 mM (inverted triangles). The continuous lines are a series of models fit to the data. Model 1 includes proton binding to the surface charge only, and no H^+ block in the pore. Model 2 eliminates the surface charge and considers only proton binding in the pore. In model 3, protons bind to the surface charge and in pore but with the same affinity. Model 4 incorporates surface charge binding and screening by Na^+ and H^+, and pore block by H^+. Models 1 and 2 are constrained subsets of model 4. (*B*) Fits of the same models to the data subset at 140 mM $[Na^+]_o$. The values for the conductances at pH 7 (triangles), 7.6 (circles) and 8 (squares) and the fits are shown to highlight the limitations of models 1–3. The sum of squared errors for models 1–4 are 0.28, 7.7, 1.2, 3×10^{-12}, respectively. The model with all the parameters (model 4) is significantly better than models 1–3 ($P < 0.001$). The entire data set at this $[Na^+]_o$ was used to generate the fits.

duction in the single-channel conductance. At pH 6.0 there is consistently a larger reduction in whole-cell conductance compared with single-channel conductance. The difference between the whole-cell and single-channel effects at the lowest pH may result from a decrease in the number of functioning channels or a reduced probability of the channel opening. Direct comparison of the effects of acidosis on gating at the whole-cell and single-channel levels is not possible because the single channels were modified to remove fast inactivation.

Differences between our data and those of Zhang and Siegelbaum may reflect the different isoforms of the channels studied, the fact that we studied expressed channels in *Xenopus* oocytes or our use of fenvalerate to remove fast inactivation. The removal of fast inactivation allowed us to focus on the changes in open-channel properties induced by $[H^+]_o$ without otherwise changing the pore properties (Fig. 2). Further, we specifically tested the role of an electrostatic mechanism for proton-induced reduction in single-channel conductance by a systematic analysis of the interaction of changing $[Na^+]_o$ and $[H^+]_o$.

To understand the molecular basis of proton inhibi-

tion of the channel, the residues involved in forming the surface charge and binding protons in the pore must be determined. Site-directed mutagenesis will be helpful in defining the amino acids involved in formation of proton binding sites. This analysis of the effect of changing the extracellular pH on heterologously expressed wild-type channels is an essential prerequisite to studying site-directed charge neutralization mutants.

This work was supported by the National Institutes of Health, R01 HL50411 (GFT), P50 HL52307 (EM), American Heart Association, Clinician Scientist Award and Passano Clinician Scientist Award of the Johns Hopkins University to J.R.B. and American Heart Association, Maryland Affiliate Fellowship to J.-P.B.

References

Backx, P.H., Marban, E., Yue, D.T. 1990. Flicker block of cardiac Na channels by Cd^{2+} protons. *Biophys. J.* **57:**298*a.* (*Abstr.*)

Backx, P.H., Yue, D.T. 1991. Proton permeation through cardiac sodium channels. *Biophys. J.* **59:**26*a.* (*Abstr.*)

Backx, P.H., Yue, D.T., Lawrence, J.H., Marban, E., Tomaselli, G.F. 1992. Molecular localization of an ion-binding site within the pore of mammalian sodium channels. *Science* **257:**248–251

Begenisich, T., Danko, M. 1983. Hydrogen block of the sodium pore in squid giant axons. *J. Gen. Physiol.* **82:**599–618

Bénitah, J.-P., Marban, E., Tomaselli, G.F. Effect of external pH on expressed sodium current. *Biophys. J.* **68:**156*a.* (*Abstr.*)

Campbell, D.T. 1982. Do protons block Na^+ channels by binding to a site outside the pore? *Nature* **298:**165–167

Chabala, L.D., Andersen, O.S. 1989. Evidence for a net negative charge near the guanidinium toxin binding site and the entrance to rat brain sodium channels. *FASEB J.* **2:***A*534 (*Abstr.*)

Colquhoun, D., Sigworth, F.S. 1983. Sitting and statistical of single-channel records. *In:* Single-Channel Recording. B. Sakmann and E. Neher, editors. pp. 191–263. Plenum Press, New York

Daumas, P., Andersen, O.S. 1993. Protons block of rat brain sodium channels. Evidence for two proton binding sites and multiple occupancy. *J. Gen. Physiol.* **101:**27–43

Drouin, H., The, R. 1969. The effect of reducing extracellular pH on the membrane currents on the Ranvier node. *Pfluegers Arch.* **313:**80–88

Grahame, D.C. 1947. The electrical double layer and the theory of electrocapillarity. *Chem. Rev.* **41:**444–501

Green, W.N., Weiss, L.B., Andersen, O.S. 1987. Batrachotoxin-modified sodium channels in planar lipid bilayers. Ion permeation and block. *J. Gen. Physiol.* **89:**841–872

Hamill, O.P., Marty, A., Neher, E., Sakmann, B., Sigworth, F.J. 1981. Improved patch-clamp technique for high-resolution current recording from cells and cell-free membrane patches. *Pfluegers Arch.* **391:**85–100

Hille, B. 1992. Ionic Channels of Excitable Membranes. pp. 341–346. Sinauer Associates, Sunderland, MA

Hille, B. 1968. Charges and potentials at the nerve surface. Divalent cations and pH. *J. Gen. Physiol.* **51:**221–236

Holloway, S.F., Salgado, V.F., Wu, C., Narahashi, T. 1989. Kinetic properties of single sodium channels modified by fenvalerate in mouse neuroblastoma cells. *Pfluegers Arch.* **414:**613–621

Horn, R. 1987. Statistical methods for model discrimination. Application to gating kinetics and permeation of the acetylcholine receptor channel. *Biophys. J.* **51:**255–263

Isom, L.L., DeJongh, K.S., Patton, D.E., Reber, B.F.X., Offord, J., Charbonneau, H., Walsh, K., Goldin, A.L., Catterall, W.A. 1992. Primary structure and functional expression of the B_1 subunit of the rat brain sodium channel. *Science* **256:**839–842

Nelder, J.A., Mead, R. 1965. A simplex method for function minimization. *Comput J.* **7:**308–313

Nuss, H.B., Chiamvimonvat, N., Pérez-García, M.T., Tomaselli, G.F., Marban, E. 1995. Functional association of the β1 subunit with human cardiac (hH1) and rat skeletal muscle (μ1) sodium channel α subunits expressed in *Xenopus* oocytes. *J. Gen. Physiol.* **106:**1171–1191

Press, W.H., Teukolsky, S.A., Vetterling, W.T., Flannery, B.P. 1992. Numerical Recipes in Fortran. The Art of Scientific Computing. 2nd ed. Cambridge University Press, New York, 340–362

Ravindran, A., Moczydlowski, E. 1989. Influence of negative surface charge on toxin binding to canine heart Na channels in planar lipid bilayers. *Biophys. J.* **55:**359–365

Sheets, M.F., Hanck, D.A. 1992. Mechanisms of extracellular divalent and trivalent cation block of the sodium current in canine cardiac Purkinje cells. *J. Physiol.* **454:**299–320

Terlau, H., Heinemann, S.H., Stühmer, W., Pusch, M., Conti, F., Imoto, K., Numa, S. 1991. Mapping the site of block by tetrodotoxin and saxitoxin of sodium channel II. *FEBS Lett.* **293:**93–96

Tomaselli, G.F., McLaughlin, J.T., Jurman, M., Hawrot, E., Yellen, G. 1991. Mutations affecting agonist sensitivity of the nicotinic acetylcholine receptor. *Biophys. J.* **60:**721–727

Trimmer, J.S., Cooperman, S.S., Tomiko, S.A., Zhou, J., Crean, S.M., Boyle, M.B., Kallen, R.G., Sheng, Z., Barchi, R.L., Sigworth, F.J., Goodman, R.H., Agnew, W.S., Mandel, G. 1989. Primary structure and functional expression of a mammalian skeletal muscle sodium channel. *Neuron* **3:**33–49

Woodhull, A.M. 1973. Ionic blockade of sodium channels in nerve. *J. Gen. Physiol.* **61:**687–708

Yatani, A., Brown, A.M., Akaike, N. 1984. Effect of extracellular pH on sodium current in isolated, single rat ventricular cells. *J. Membrane Biol.* **78:**163–168

Zhang, J.-F., Siegelbaum, S.A. 1991. Effects of external protons on single cardiac sodium channels from guinea pig ventricular myocytes. *J. Gen. Physiol.* **98:**1065–1083